Energy Equip. Sys./ Vol. 5/No2/June 2017/ 95-113

ENERGY EQUIPSYS

Energy Equipment and Systems

http://energyequipsys.ut.ac.ir
www.energyequipsys.com

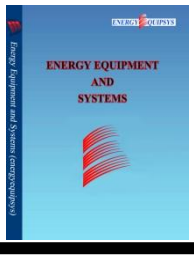

Exergy , economy and pressure drop analyses for optimal design of recuperator used in microturbine

Authors

Pedram Hanafizadeh [a*]
Peyman Maghsoudi [a]

[a] Center of Excellence in Design and Optimization of Energy Systems, School of Mechanical Engineering, College of Engineering, University of Tehran, P. O. Box: 11155-4563, Tehran, Iran

Article history:

Received : 4 February 2016
Accepted : 18 April 2016

ABSTRACT

The optimal design of a plate-fin recuperator of a 200-kW microturbine was studied in this paper. The exergy efficiency, pressure drop and total cost were selected as the three important objective functions of the recuperator. Genetic Algorithm (GA) and Non-dominated Sorting Genetic Algorithm (NSGA-II) were respectively employed for single-objective and multi-objective optimizations. By optimizing the objective functions via the single-objective optimization approach, the optimum values of exergy efficiency, pressure drop and total cost were found to be 0.966, 0.846 kPa, and 302,075$ respectively, representing the best solutions obtained from 20 iterations in GA. The cases considered for bi-objective optimizations were exergy efficiency-total cost, exergy efficiency-pressure drop and total cost-pressure drop pairs for which Pareto-optimal fronts were obtained, revealing the confliction between the two objectives in each pair. Later, a three-objective optimization was undertaken to simultaneously maximize exergy efficiency while minimizing pressure drop and total cost; the results were presented in a three-dimensional Pareto-optimal front. Moreover, the results of the multi-objective optimizations (i.e. three-objective and bi-objective optimizations) were compared with those of the single-objective one. The comparisons indicated a very good match between the multi-objective and the single-objective optimum values when it came to exergy efficiency and total cost; for pressure drop, however, significant differences were observed. Eventually, a decision-making procedure was employed for the Pareto-fronts of multi-objective optimization to find the final optimal solution.

Keywords: Recuperator, Microturbine, Genetic Algorithm, Multi-Objective Optimization, Decision-Making.

1. Introduction

Microturbines refer to small-scale power generation devices like fuel cells and reciprocating engines [1]. Running in a thermodynamic cycle, a microturbine consists of a compressor, a combustion chamber, and a turbine that work together to generate power,as shown in Fig. 1(a). The cycle net output power ranges from 5 to 200 kW [2], and as it suffers from low efficiency, there is a need to follow a proper approach to increase its efficiency. Figure 1(b) illustrates a microturbine cycle in which a recuperator is used to increase the efficiency by reducing fuel consumption. On the other hand, an exhaust heat recovery recuperator is

*Corresponding author: Pedram Hanafizadeh
Address: Center of Excellence in Design and Optimization of Energy Systems, School of Mechanical Engineering, College of Engineering, University of Tehran, P. O. Box: 11155-4563, Tehran, Iran
E-mail address: Hanafizadeh@u.ac.ir

necessary to obtain 30% or higher electrical efficiency for a microturbine [3]. In contrast, a recuperator-derived pressure drop at both the cold and hot sides increases the cycle pressure drop that results in reduced net output power of the microturbine. In economic terms, the share of the recuperator in the total capital cost of a microturbine package is seen to reach up to 30% [4]. According to the above explanations, technical and economical optimizations can be seen as requirements for the recuperator used in a microturbine cycle.

Plate-fin heat exchangers are extensively employed in many industrial applications, such as microturbines, chemical, petroleum, cryogenic and aeronautical applications; this wide range of applications is related to the high effectiveness, compactness, low weight and small volume of plate-fin heat exchangers [5]. Figure 2 shows a plate-fin heat exchanger of counter-flow arrangement. Different types of fins are used in the plate-fin heat exchanger; here are a number of the more common types: plain, wavy, offset strip, louvered, perforated and pin fins. Applying fins on both sides can increase the obtained heat transfer rate due to the extended heat transfer area and the interruption of boundary layer growth. Figure 3 shows a rectangular offset strip fin—the fin type investigated in this paper.

Compact heat exchangers are widely studied in the literature [7-8]. The heat transfer and flow resistance characteristics of rectangular offset strip fins are well reported by Manglic and Bergles. They presented some correlations for f (friction factor) and j (Colburn number) in the form of single continuous expressions covering all regimes of flow [9]. Traverso and Massardo

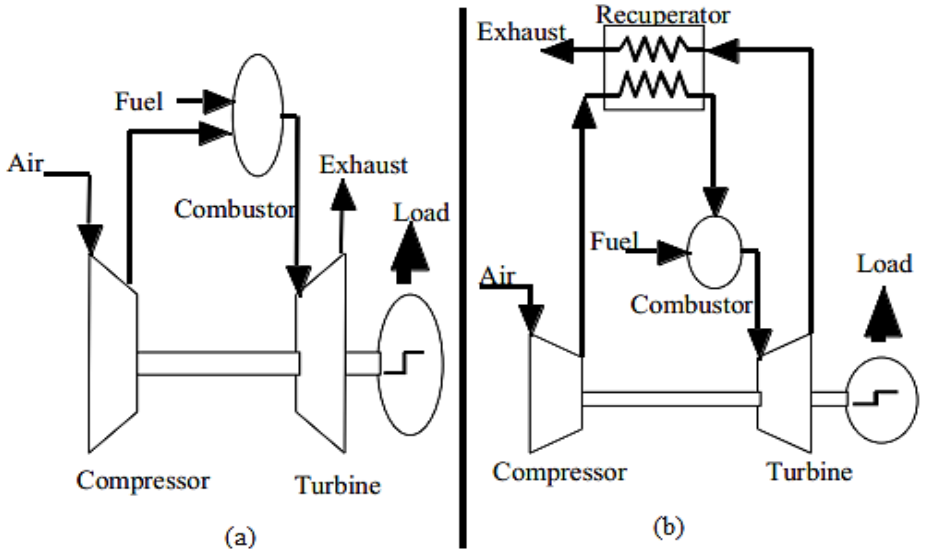

Fig.1. Schematic diagram of microturbine cycle: (a) Simple cycle, (b) Recuperated cycle [1]

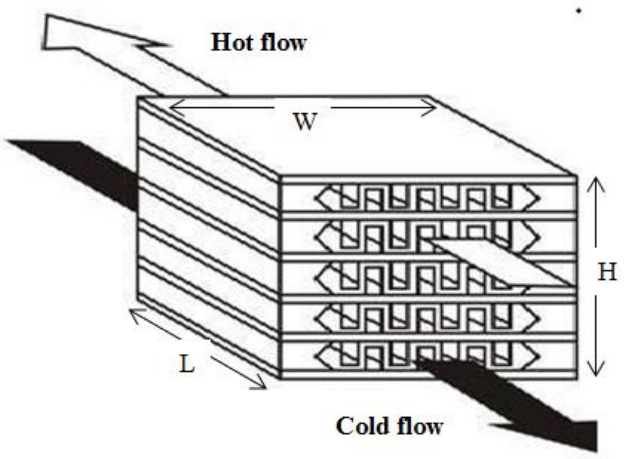

Fig.2. Plate-fin heat exchanger with counter-flow arrangement

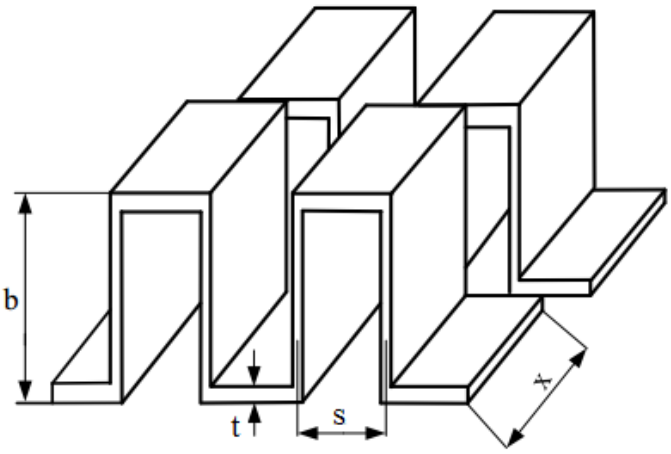

Fig.3. Core of rectangular offset strip fin [6]

implemented optimization of microturbine recuperators from technical and economic perspectives. The optimizations has been modified to follow a new approach undertaken in a software called CHEOPE (compact heat exchanger optimization and performance evaluation) [4]. Qiuwang *et al.* applied GA to optimize a primary surface of the recuperator used in 100 kW microturbine [3]. Xie and Sunden proposed an optimization method for a plate-fin heat exchanger, by considering total annual cost and total volume as two separate objectives, where a GA was used for optimizations. They chose three shape parameters as decision variables before solving the optimization problem with or without pressure drop constraints, respectively [5]. Liu and Cheng optimized the primary surface recuperator from heat transfer performance, exchanger weight and pressure loss standpoints [10]. Peng and Ling studied a plate-fin heat exchanger with offset strip fins to optimize its performance using neural networks and GA [11]. Using NSGA-II, Sanaye and Hajabdollahi optimized the design parameters of a plate-fin heat exchanger from the thermoeconomic point of view [12]. A multi-objective optimization approach was followed by Ahmadi *et al.* to minimize cost and entropy generation of a plate-fin heat exchanger, simultaneously [13]. Najafi *et al.* used NSGA-II to obtain the optimal performance to be delivered by a heat exchanger with offset strip fins. Their objective functions were those of heat transfer rate and total annual cost [14].

In this article, once finished with thermo-hydraulic modeling of a microturbine plate-fin recuperator, single - objective and multi-objective optimizations are performed to maximize recuperator exergy efficiency while minimizing its total cost and pressure drop. Single-objective optimizations are carried out for each objective function with the optimal solutions been obtained using GA. Then, NSGA-II is used to undertake three bi-objective and one three-objective optimizations on the mentioned functions with Pareto-optimal fronts provided for each case of multi-objective optimization. Afterward, bi-objective optimizations are compared, in terms of performance (i.e. maximum exergy efficiency and minimum total cost and pressure drop), to the three single-objective optimizations. Finally, a decision-making method is presented to evaluate final optimal solution for the designs on Pareto-front in multi-objective optimization.

Nomenclature

a	thickness of separation plate, m
A	overall heat transfer area, m^2
A_{cell}	total heat transfer area for one fin, m^2
A_{fin}	fin heat transfer area, m^2
A_{front}	recuperator frontal area, m^2
A_w	wall heat transfer area, m^2
$A_{min,fl}$	minimum free flow area, m^2
b	fin height, m
Cp	specific heat capacity, $^{J}/_{kgK}$
c^*	ratio of heat capacity rate

C	heat exchanger cost coefficient, $^{W}/_{K}$
$Cost$	total cost, $
$c_{ope,A}$	first year operational cost, $
$c_{ope,p}$	present value of operational cost, $
$c_{purchase}$	purchase cost, $
$c_{Capital}$	capital cost, $
$c_{Maintenance}$	maintenance cost, $
D_h	hydraulic diameter, m
ex	specific exergy rate, $^{W}/_{kg}$
$Ex_{D,R}$	recuperator exergy destruction rate, W
f	friction factor
f^*	inflation rate, %
G	mass flux, $^{kg}/_{m^2 s}$
h	convective heat transfer coefficient, $^{W}/_{m^2 K}$
H	recuperator height
i	interest rate, %
j	colburn number
K_e	exit pressure loss coefficient
K_c	entrance pressure loss coefficient
k_{el}	price of electrical energy, $^{\$}/_{kWh}$
k_{fin}	fin thermal conductivity coefficient, $^{W}/_{mK}$
k_w	wall thermal conductivity coefficient, $^{W}/_{mK}$
L	recuperator flow stream length, m
LHV	fuel lower heating value, $^{kJ}/_{kg}$
m	mass flow rate, $^{kg}/_{s}$
n	recuperator operation period, year
N_p	number of passage for hot fluid
NTU	number of transfer unit
P	pressure, kPa
$P_{o,cycle}$	cycle pressure outlet, kPa
Pr	Prandtl number
Q	rate of heat transfer, W
R_f	fouling factor, $^{m^2 K}/_{W}$
Re	Reynolds number
s	fin pitch, m
St	Stanton number
T	temperature, K
T_{TIT}	turbine inlet temperature, K
T_0	reference temperature, K
t	fin thickness, m
UA	overall heat transfer coefficient, $^{W}/_{K}$
V_p	volume between plate, m^3
W	recuperator width, m
x	offset length, m

Greek abbreviation

β	heat transfer area per unit volume, $^{m^2}/_{m^3}$
ΔT_m	corrected temperature, K
ΔP	pressure drop, kPa
ε	recuperator energy efficiency, %
$\eta_{ex,r}$	recuperator exergy efficiency, %
η_{fin}	single fin efficiency, %
η_s	overall fin efficiency, %
η_{comp}	compressor efficiency, %
η_{th}	cycle thermal efficiency, %
η_{ex}	cycle exergy efficiency, %
ϑ_m	mean specific volume, $^{m^3}/_{kg}$
ρ	density, $^{kg}/_{m^3}$
σ	ratio of minimum free flow area to frontal area
τ	hours of operation per year, hour

Subscripts

a	air
c	Cold
g	gas
h	Hot
i	Inlet
o	outlet

2.Modelling of the system

This section offers the necessary equations for calculating recuperator energy efficiency, pressure drop, exergy efficiency and cost. Considering the non-stationary nature of recuperator energy and exergy efficiencies, which implies that the fuel mass flow rate would exhibit some variations, it is essential to link the heat exchanger design code to a thermodynamic analysis of the cycle (i.e. solving the energy equation in the combustion chamber).

2.1.Heat transfer equations

The geometrical characteristics of a plate-fin heat exchanger with offset strip fins and counter-flow arrangements are provided in Table 1 [15].
Mass flux and Reynolds number are calculated as follows:

$$G = \frac{m}{A_{\min\_flow}} \tag{1}$$

$$\mathrm{Re} = \frac{GD_h}{\mu} \tag{2}$$

Colburn number and friction factor of the offset strip fins are defined in Eqs. (13) and (14), by Manglik and Bergles [9], as follows:

$$j = 0.6522\, Re^{-0.5403}\alpha^{-0.1541}\delta^{0.1499}\gamma^{-0.0678}[1 + (5.269 \times 10^{-5} Re^{1.34}\alpha^{0.504}\delta^{0.456}\gamma^{-1.055}]^{0.1} \tag{3}$$

$$f = 9.6243 Re^{-0.7422}\alpha^{-0.1856}\delta^{0.3053}\gamma^{-0.2659}[1 + 7.669 \times 10^{-8} Re^{4.429}\alpha^{0.92}\delta^{3.767}\gamma^{0.236}]^{0.1} \tag{4}$$

The above equations are usable for $120 < Re < 10^4$, $0.134 < \alpha < 0.997$, $0.012 < \delta < 0.048$, $0.041 < \gamma < 0.121$, where $\alpha = {}^{s}/_{b}$, $\delta = {}^{t}/_{x}$, $\gamma = {}^{t}/_{s}$.

Stanton number and convective heat transfer coefficient are computed from:

$$\mathrm{St} = \frac{\mathrm{j}}{\mathrm{Pr}^{\frac{2}{3}}} \tag{5}$$

$$h = GCp\mathrm{St} \tag{6}$$

Single-fin efficiency (η_{fin}) is calculated as follows:

$$\eta_{fin} = \frac{tgh(Ml)}{Ml} \tag{7}$$

where

$$M = \sqrt{\frac{2h}{k_{fin}t}} \tag{8}$$

Table 1. Recuperator surface geometrical characteristics

Equations	No	Remarks
$A_f = 2x(b-t) + 2t(b-2t) + st$	1	One fin heat transfer area
$A_{cell} = 2x(b-t) + 2x(s-t) + 2t(b-t) + st$	2	Total heat transfer area for one fin
$A_{front} = HW$	3	Frontal area
$N_p = \frac{H-b-2a}{2b+2a}$	4	Number of passage for hot fluid
$V_{p,c} = LWb(N_p + 1)$	5	Volume between plates for cold fluid
$V_{p,h} = LWbN_p$	6	Volume between plates for hot fluid
$\beta = \frac{A_{cell}}{sbx}$	7	Heat transfer area per unit volume
$A = \beta V_p$	8	Total heat transfer area
$D_h = \frac{4x(s-t)(b-t)}{2[(s-t)x + (b-t)x + (b-t)t] + (s-t)t - t^2}$	9	Hydraulic diameter
$A_{min,flow} = \frac{D_h A}{4L}$	10	Minimum free flow area

and

$$l = 0.5b - t \tag{9}$$

The overall surface efficiency (η_s) can be computed via the following equation:

$$\eta_s = 1 - \frac{A_{fin}}{A_{cell}}(1 - \eta_{fin}) \tag{10}$$

Overall heat transfer coefficient (UA_{tot}) is calculated from the following correlation [16]:

$$UA = \frac{1}{\left[\frac{1}{h_c \eta_{s,c} A_c} + \frac{1}{h_h \eta_{s,h} A_h} + \frac{a}{A_w k_w} + \frac{R_{f,c}}{A_c} + \frac{R_{f,h}}{A_h}\right]} \tag{11}$$

Number of transfer units (NTU) and ratio of heat capacity rates (c^*) are defined as follows:

$$NTU = \frac{UA}{c_{min}} \quad , \quad c_{min} = \min\{m_c Cp_c, m_h Cp_h\} \tag{12}$$

$$c^* = \frac{c_{min}}{c_{max}} \quad , \quad c_{max} = \max\{m_c Cp_c, m_h Cp_h\} \tag{13}$$

The energy efficiency of a heat exchanger with counter flow arrangement is calculated as follows [15]:

$$\varepsilon = \frac{1 - exp[-NTU(1 - c^*)]}{1 - c^* exp[-NTU(1 - c^*)]} \tag{14}$$

The energy equation in the combustion chamber is defined as follows [17]:

$$m_a Cp_a (T_{o,a} - T_0) + m_{fuel} LHV = m_g Cp_g (T_{TIT} - T_0) \tag{15}$$

where

$$Q = \varepsilon c_{min} (T_{i,h} - T_{i,c}) \tag{16}$$

and

$$T_{o,c} = T_{i,c} + \frac{Q}{m_c Cp_c} \, , \quad T_{o,h} = T_{i,h} - \frac{Q}{m_h Cp_h} \tag{17}$$

The new values of energy efficiency and fuel mass flow rate are compared to their initial guesses, so as to obtain solutions with high accuracy in terms of these parameters.

2.2.Pressure drop calculation

The pressure drop in a compact heat exchanger can be calculated as follows [4]:

$$\frac{\Delta P}{P_i} = \frac{4G^2 \vartheta_m f L}{2D_h P_i} + \frac{G^2}{2\rho_i P_i}\left(\frac{\rho_i}{\rho_o} - 1\right) + \frac{G^2}{2\rho_i P_i}(1 - \sigma + K_c) + \frac{G^2}{2\rho_o P_i}(1 - \sigma + K_e) \tag{18}$$

$$\frac{\Delta P}{P_i} = \frac{4G^2 \vartheta_m f L}{2D_h P_i} + \frac{G^2}{2\rho_i P_i}\left(\frac{\rho_i}{\rho_o} - 1\right) + \frac{G^2}{2\rho_i P_i}(1 -$$

where σ is the ratio of minimum free flow area to frontal area and ϑ_m, K_c, and K_e are respectively the mean specific volume, the entrance and the exit pressure loss coefficients.

First, the cold side pressure drop is obtained from the above equation, and then, according to the obtained value (for the cold side pressure drop), the hot side inlet pressure is calculated from the pressure equations in the cycle component. Finally, the recuperator hot side pressure drop is estimated by Eq. (28).

2.3.Exergy analysis

Exergy refers to the maximum producible amount of work by a system or a substance flow as it equilibrates with a reference environment's temperature, pressure, and chemical composition [13]. Exergy is divided into four components: physical, chemical, kinetic and potential [17]. Since the kinetic and the potential components of exergy are assumed to be negligible and the chemical exergy is only important for combustion processes [17], the physical exergy remains the only type of exergy that is important for a recuperator. Combining the first and the second laws of thermodynamics, the exergy balance equation is established as follows [17]:

$$Ex_Q + \sum_i m_i ex_i = \sum_e m_e ex_e + Ex_w + Ex_D \tag{19}$$

where Ex_Q and Ex_w are related to the exergies of heat transfer and work. These can be calculated as follows:

$$Ex_Q = \left(1 - \frac{T_0}{T_i}\right) Q_i \tag{20}$$

$$Ex_w = W \tag{21}$$

As the recuperator is isolated and does not perform any work, the values of Ex_Q and Ex_w are equal to zero [13].

Physical exergy (ex_{ph}) and exergy destruction of the recuperator are computed from the following equations [17]:

$$ex = ex_{ph} = (h - h_0) - T_0(s - s_0) \quad (22)$$

$$Ex_{D,R} = \sum_i m_i ex_i - \sum_e m_e ex_e \quad (23)$$

The exergy efficiency of a recuperator is defined as follows [17]:

$$\eta_{ex,r} = 1 - \frac{Ex_{D,R}}{\sum_{i,R} Ex} \quad (24)$$

The necessary equations for calculating energy and exergy efficiencies of the cycle are obtained from Ref. [17].

2.4.Cost estimation

The capital cost, operational cost and maintenance cost of a recuperator are considered the three major components when estimating the total cost of the recuperator [14].

The recuperator capital cost is related to its manufacturing phase. The ESDU (Engineering Sciences Data Unit) method is employed to estimate the purchase cost, which is presented in terms of $Q/\Delta T_m$ [18]. The values of $Q/\Delta T_m$ and purchase cost ($c_{purchase}$) are obtained from:

$$\frac{Q}{\Delta T_m} = c_{min} NTU \quad (25)$$

and

$$c_{purchase} = C\left(\frac{Q}{\Delta T_m}\right) \quad (26)$$

where C is the plate-fin recuperator cost in terms of $Q/\Delta T_m$ [18].

The recuperator capital cost is computed as follows [19]:

$$c_{Capital} = 1.47\, c_{purchase} \quad (27)$$

The maintenance cost is expressed as a fraction of the purchase cost, as follows:

$$c_{Maintenance} = 0.03\, c_{purchase} \quad (28)$$

The cost of electricity consumed by the compressor to compensate for the recuperator pressure drop is considered as an operational cost, which is calculated as follows [6, 20]:

$$c_{ope,\mathrm{A}} = \left(k_{el}\tau \frac{\Delta Pm}{\eta_{comp}\rho}\right)_{\mathrm{c}} + \left(k_{el}\tau \frac{\Delta Pm}{\eta_{comp}\rho}\right)_{\mathrm{h}} \quad (29)$$

$$c_{ope,\mathrm{p}} = c_{ope,\mathrm{A}}\left(\frac{1-(1+f^*)^n(1+i)^{-n}}{i-f^*}\right) \quad (30)$$

In the above equations, $c_{ope,\mathrm{A}}$ and $c_{ope,\mathrm{p}}$ are the first year operational cost and the present value of operational cost respectively. The present value of the recuperator total cost is defined as follows:

$$Cost = c_{ope,\mathrm{p}} + c_{Maintenance} + c_{Capital} \quad (31)$$

3.Optimization

3.1.Single-objective and multi-objective optimizations

Over the past decade, optimization algorithms have been widely employed mainly for energy system applications [21]. Depending on the assigned objective(s), either single-objective or multi-objective optimizations can be used. A single-objective optimization includes maximization or minimization of only one objective function; multi-objective optimization, however, involves optimization (either maximization or minimization) of at least two objective functions simultaneously. A multi-objective optimization is defined as follows [22]:

$$min\ F(X) = [f_1(X), f_2(X), \dots, f_n(X)]^T \quad (32)$$

Subjected to

$$g_i(X) \le 0, \quad \forall\, i = 1,2,,\dots,m \ \ and \ \ h_j(X) \le 0 \quad \forall\, j = 1,2,,\dots,M \quad (33)$$

$$x_{k,min} \le x_k \le x_{k,max} \quad (34)$$

In the above equations, X, $F(X)$, $g_i(X)$ and $h_j(X)$ represent the decision variables vector, the objective functions vector, the inequality and the equality constraints respectively; $x_{k,min}$ and $x_{k,max}$ are the lower and the upper bounds of the decision variables respectively.

For the optimization constraints to be satisfied, a penalty function is applied as follows:

$$Minimize \quad f(x) = f(x) + \sum_{j=1}^{m} R_1 (c_j(x))^2 \qquad (35)$$

where R_1 is a constant much greater than f, and c represents the violation criteria of the constraints.

3.2.Optimization algorithm

Contrary to the traditional optimization approaches, GA is an optimization approach that does not require gradient or function differentiations [23]. It is a semi-stochastic method inspired by the natural selection concept introduced by Darwin's theory [24] and then developed by Holland [25].

Schaffer was the first to propose a multi-objective GA called vector evaluated GA (VEGA) [26]. Then, Srinivas and Deb proposed NSGA [27] before it was modified by Deb et al. to develop NSGA-II [28, 29]. The different steps followed via GA and NSGA-II can be expressed as follows:

1. Initialize population individuals
2. Check feasibility of each individual
3. Compute the fitness of each individual
4. Order the population
5. Perform the selection, crossover and mutation processes
6. Update the population for the next generation

In GA, the fourth step (ordering the population) is performed on the basis of the fitness value. NSGA-II, however, undertakes the two later steps to establish the ordering of the population:

a. Classify the individuals based on non-dominated sort
b. Rank the individuals based on crowding distance

Figure 4 shows the flowcharts of GA and NSGA-II.

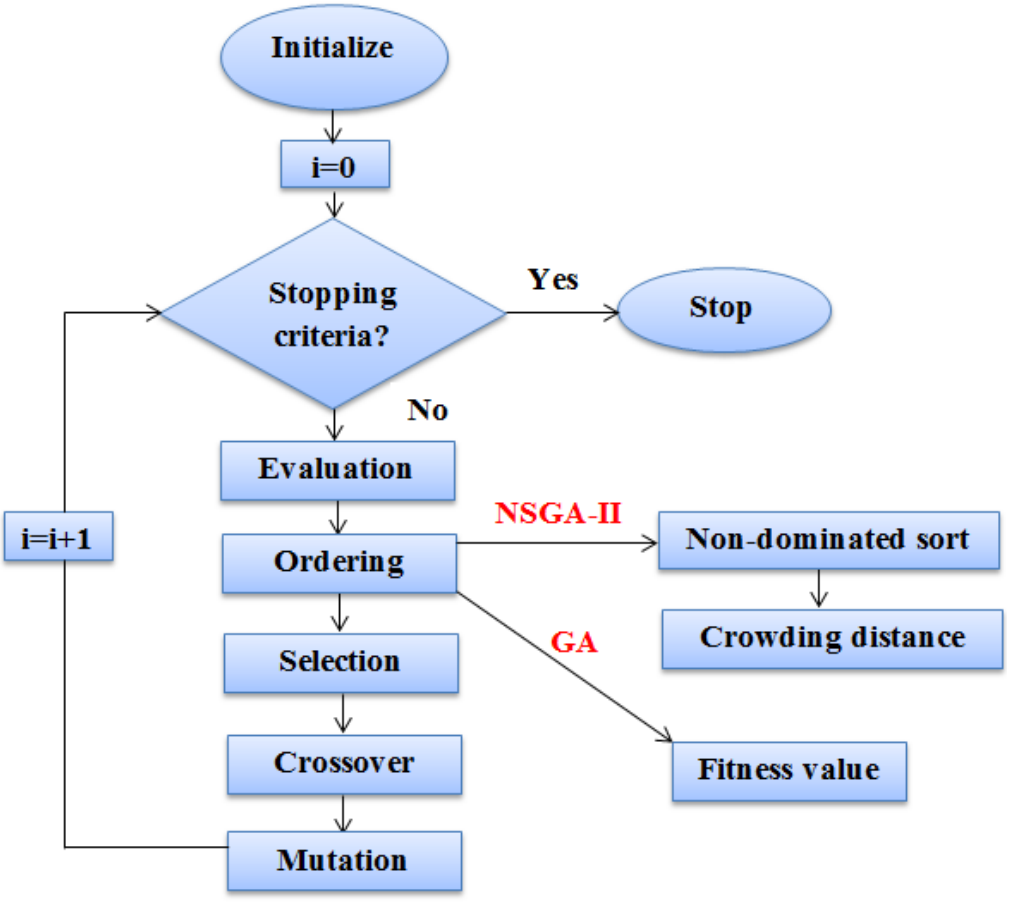

Fig. 4. Flowchart of GA and NSGA-II

3.3.Objective functions, design parameters and constraints

In the present study, the recuperator exergy efficiency, the pressure drop and the total cost are considered as the three objective-functions for single-objective and multi-objective optimizations. Accordingly, fin pitch (s), fin height (b), recuperator flow length (L), recuperator width (W), and recuperator height (H) are taken as the six decision variables to be used for optimizations. The ranges of the decision variables are presented in Table 2. The constraints and parameters of GA and NSGA-II incorporated in the optimization algorithm are listed in Table 3.

4.Case study

In this paper, recuperator optimization was performed for a 200 kW microturbine. The required information on the considered microturbine and the economic assumptions used in the course of optimization are summarized in Table 4.Fluid properties and thermal conductivity of fin were considered the functions of temperature. The recuperator plate and the fin were assumed to be 0.2 mm and 0.1 mm thick respectively.

5.Results and discussion

5.1.Model verification

In this subsection, the recuperator thermo-hydraulic modelling results are compared to those of the reference [15]. Table 5 compares the recuperator efficiency as well as the hot and cold side pressure drops in the present study with those of the reference [15] under the same operating conditions.

Table 2. Range of decision variables

Variables	Lower bound	Upper bound
$\mathbf{S(m)}$	10^{-3}	3×10^{-3}
$\mathbf{b(m)}$	2×10^{-3}	10×10^{-3}
$\mathbf{x(m)}$	3×10^{-3}	6×10^{-3}
$\mathbf{L(m)}$	0.1	1
$\mathbf{W(m)}$	0.1	1
$\mathbf{H(m)}$	0.1	1

Table 3. Constraints and parameters applied in GA and NSGA-II algorithms for the optimization

Parameter	Value
Population size	25
Generation	5000
Crossover fraction	0.8
Pareto front population fraction	0.35
Average change in the spread of	$< 10^{-6}$
Average change in the fitness value	$< 10^{-6}$
Pressure drop	$P_{o,cycle} \geq 101kPa$
Reynolds number	$500 < Re < 1500$
Recuperator efficiency	$\varepsilon \geq 0.7$

Table 4. Recuperator and microturbine operation conditions and economic data

Parameter	Unit	Value
Air mass flow rate	Kg/s	1.286
Cold side inlet pressure	kPa	404.1
Cold side inlet temperature	K	469.95
Hot side inlet temperature	K	1009.65
Turbine inlet temperature	K	1312.15
Fuel lower heating value(LHV)	kJ/kg	42557
Compressor pressure ratio	-	4
Turbine pressure ratio	-	3.65
Combustor pressure drop		4
Reference temperature	K	298.15
Interest rate	%	10
Inflation rate	%	20
recuperator operation period	year	10
price of electrical energy	$/kWh	0.000125
hours of operation per year	hour	6000
compressor efficiency	%	76

Table 5. Modeling verification results

Output Variables	Unit	Ref. [4]	Present work	Difference (%)
Efficiency	-	0.8381	0.8263	1.41
Hot side pressure drop	kPa	9.05	8.503	6.04
Cold side pressure drop	kPa	8.757	8.237	5.94

5.2.Optimization results

The optimization problem was solved for the plate-fin recuperator with offset strip fin and counter-flow arrangement. Single-objective optimization, bi-objective optimization and three-objective optimization were undertaken to minimize the total cost and the pressure drop as well as to maximize the exergy efficiency of the microturbine recuperator.

5.2.1.Single-objective optimization

The single-objective optimization of GA was applied to separately minimize the recuperator total cost and the pressure drop and to maximize its exergy efficiency. To find a solution with a good accuracy, the optimization algorithm was iterated 20 times.

Figure 5 illustrates that when optimizing the recuperator exergy efficiency using GA, the parameter was converged after 56 generations. The optimum value of exergy efficiency was found to be 0.966 with a total cost of 326,967.8 $ under 6.061kPa of pressure drop. The optimal solution was labelled with the letter A.

Figure 6 shows that while optimizing the recuperator total cost using GA, the solution converged at the 51st generation. The optimum value of the total cost was found to be 302,075 $ with the exergy efficiency and the pressure drop being 0.932 and 2.36kPa respectively. The optimal solution was labelled with the letter B.

Figure 7 shows that, when optimizing the recuperator pressure drop using GA, the solution converged at the 85th generation. The

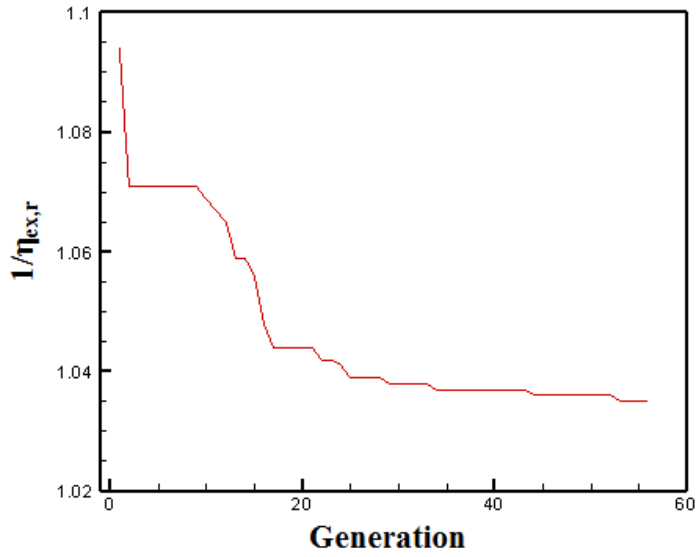

Fig. 5. Convergence of GA for maximum exergy efficiency

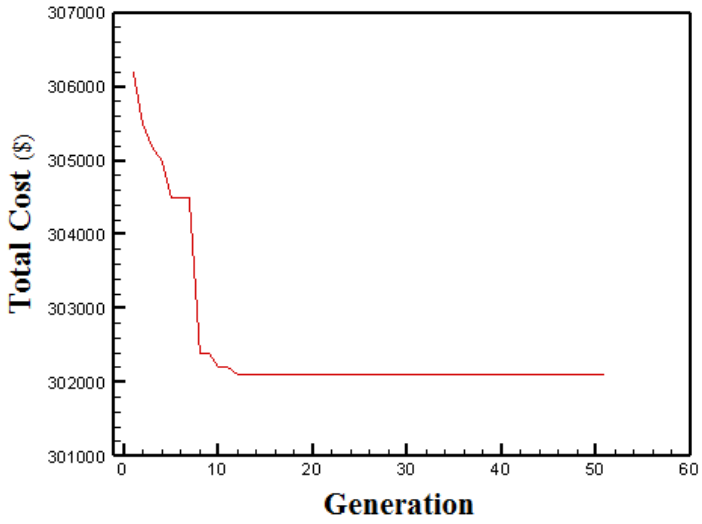

Fig. 6. Convergence of GA for minimum total cost

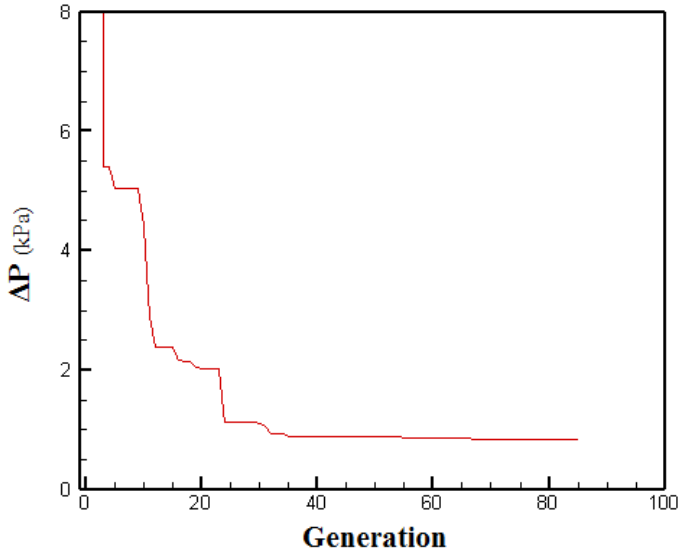

Fig.7. Convergence of GA for minimum pressure drop

optimum value of the pressure drop was found to be 0.846kPa with the exergy efficiency and the total cost being 0.894 and 324,896.6$ respectively. The optimal solution was labelled with the letter C.

The geometrical characteristics and the single-objective optimization results are respectively presented in Tables 6 and 7.

5.2.2.Bi-objective optimization

With the recuperator exergy efficiency, the total cost and the pressure drop being considered as the objective functions for the bi-objective optimization phase, so the three bi-objective optimization problems could be solved. The Pareto-optimal fronts were obtained for each optimization problem, so as to demonstrate the confliction(s) between the pairs of objectives. It can be concluded that a change in the geometry of the recuperator that may seem appropriate in terms of one objective, can be rendered unfavourable in terms of another objective, and vice versa; this suggests that multi-objective optimization would be a suitable approach to analyse this problem.

The corresponding Pareto-optimal front to the recuperator exergy efficiency and its total cost, are shown in Fig. 8. As can be observed, the optimization constraints are satisfied at the design points D, E and F. The maximum exergy efficiency occurs at the design point F (0.964) and the minimum total cost is incurred at the design point D (302,079.1$).

Figure 9 shows the corresponding Pareto-optimal front to the recuperator exergy efficiency and its pressure drop. Here the

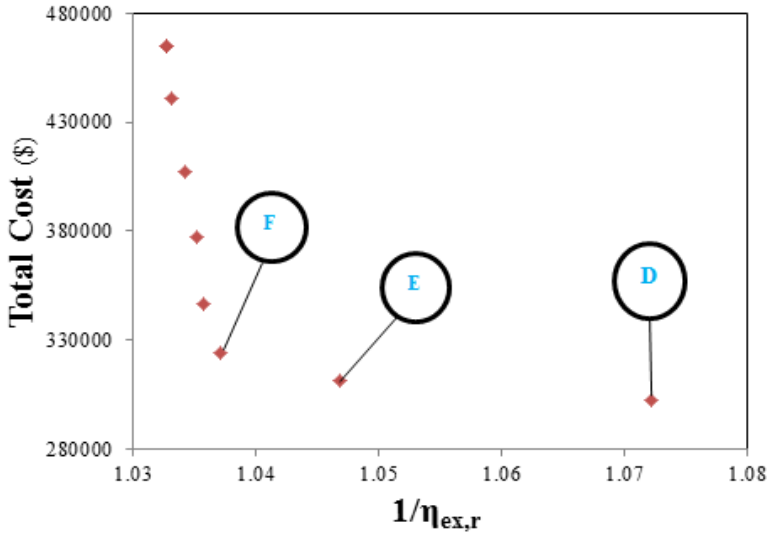

Fig. 8. Pareto-optimal front for exergy-economic optimization

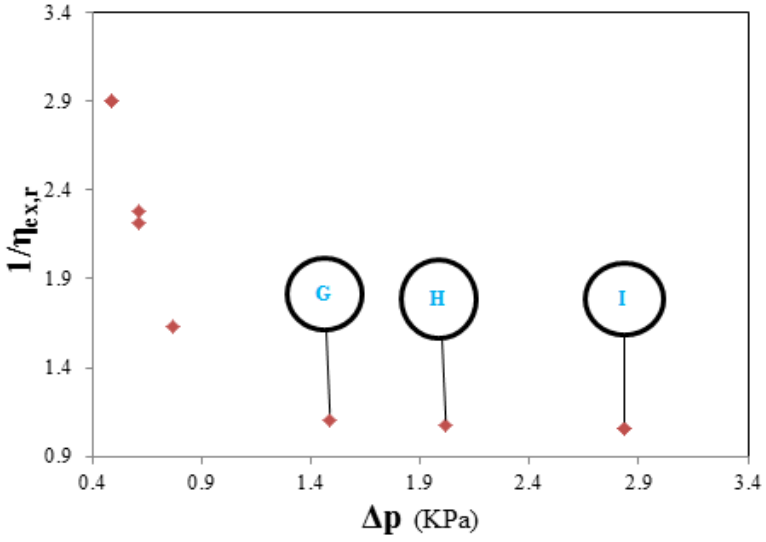

Fig. 9. Pareto-optimal front for exergy-hydraulic optimization

optimization constraints are met at the design points I, H, and G. Occurring at the design point G, the best hydraulic performance, in terms of pressure drop, was found to be 1.485 kPa. The corresponding maximum exergy efficiency was that of the design point I (0.949).

Figure 10 illustrates the corresponding Pareto-optimal front to the recuperator total cost and its pressure drop. In this case, J and K are the design points at which the optimization constraints are satisfied. The minimum pressure drop occurred at the design point K (1.283 kPa), with the best economic performance, in terms of total cost, being recorded at the design point J (302,076$).

The geometrical characteristics and the optimal results of the bi-objective optimal design points are respectively presented in Tables 6 and 7.

5.2.3.Three-objective optimization

For a recuperator with good thermodynamic, hydraulic and economic performances, the three-objective optimization using NSGA-II was conducted to minimize the total cost and the pressure drop and to maximize the exergy efficiency.

Figure 11 illustrates the corresponding 3-D set of Pareto-optimal front to the three-objective optimization. According to the considered optimization constraints, L represents the only acceptable design point. The best thermodynamic (in terms of exergy efficiency), hydraulic (in terms of pressure drop) and economic (in terms of total cost) performances were those corresponding to the design point L (0.933, 2.609 kPa, and 302,082.8$ respectively). The geometrical characteristics and the optimal results of the

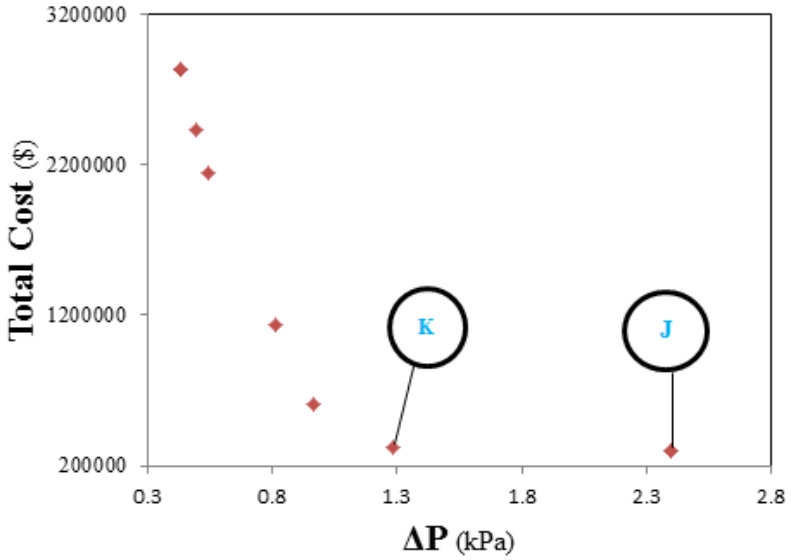

Fig. 10. Pareto-optimal front for economic-hydraulic optimization

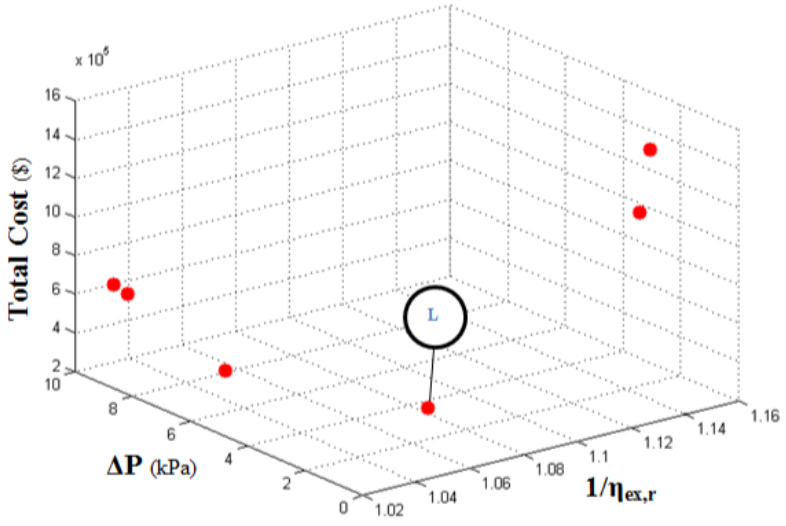

Fig. 11. Pareto-optimal front for three-objective optimization

Table 6. Geometrical characteristics for optimal designs

Design	S (m)	b (m)	x (m)	L_c (m)	L_h (m)	L_n (m)
A	0.002352	0.004125	0.003364	0.978836	1	0.462368
B	0.002377	0.009565	0.004961	0.666429	0.555927	0.931137
C	0.002439	0.007053	0.005662	0.227656	0.568799	0.913237
D	0.002102	0.008682	0.005994	0.579856	0.74534	0.663939
E	0.002134	0.005851	0.005582	0.86458	0.822371	0.534538
F	0.002361	0.003854	0.004947	0.989165	0.869925	0.497827
G	0.00242	0.009515	0.005742	0.419759	0.751632	0.667243
H	0.002414	0.009245	0.005728	0.64612	0.584973	0.930712
I	0.002402	0.009244	0.005641	0.950726	0.581626	0.96681
J	0.002412	0.009869	0.003521	0.646417	0.754754	0.712983
K	0.002417	0.009923	0.003556	0.316194	0.759434	0.68027
L	0.002078	0.005552	0.005987	0.462596	0.57192	0.77264

Table 7. Optimal results for each optimization

Design	Cost ($)	ε	ΔP (kPa)	$\eta_{ex,r}$	η_{th}	η_{ex}
A	326967.8	0.941408	6.061116	0.965799	0.391031	0.367202
B	302075	0.8558	2.360096	0.93249	0.348088	0.326876
C	324896.6	0.70002	0.845718	0.893777	0.2839	0.266599
D	302079.1	0.856211	2.490781	0.932628	0.347952	0.326748
E	311510.8	0.916682	4.689644	0.955211	0.378149	0.355105
F	323950.3	0.937935	6.025052	0.964262	0.388655	0.364971
G	309452.3	0.776049	1.484859	0.909379	0.311726	0.292729
H	302065.7	0.854975	2.013476	0.932214	0.34858	0.327338
I	306665.3	0.901515	2.830932	0.949116	0.373823	0.351042
J	302076	0.856146	2.395281	0.932606	0.348172	0.326955
K	317646.9	0.732009	1.282647	0.89961	0.294495	0.276548
L	302082.8	0.85628	2.60852	0.932651	0.347688	0.3265

the design point are presented in Tables 6 and 7, respectively.

5.3. Comparison between single-objective and multi-objective optimization results

Reported in Tables 8 and 9, the results of single-objective optimizations (with exergy efficiency, total cost and pressure drop been separately taken as the single objective function) were compared to those of multi-objective optimizations. The highlighted cells show the ability of multi-objective results to return the results of single-objective optimization. As shown in these cells, the maximum and minimum difference between the single – objective and multi - objective approaches are 3.432% and 0.159% for exergy efficiency, and 0.003% and 0.001% for total cost respectively. These values indicate that the multi-objective optimizations succeeded in reaching the results of the single-objective, with a high level of accuracy, in terms of exergy efficiency and total cost; for the pressure drop, however, higher discrepancies were observed (minimum and maximum differences of 51.664% and 208.439% respectively).

5.4.Evaluation of final optimal solutions

The optimum solution can be selected on the basis of the decision-maker criteria; however, each point on a Pareto-optimal front represents a potential optimum design. A normalization method was employed in this

Table 8. Comparisons of single-objective results with bi-objective optimal designs

Term	$\eta_{ex,r}$	Total Cost ($)
Bi-objective(D point)	0.932628	302079.1
Single-objective(cost)	0.93249	302075
Difference (%)	0.0148	**0.001**
Bi-objective(F point)	0.964262	323950.3
Single-objective($\eta_{ex,r}$)	0.965799	326967.8
Difference (%)	**0.159**	0.931
Term	$\eta_{ex,r}$	ΔP (kPa)
Bi-objective(G point)	0.909379	1.484859
Single-objective(ΔP)	0.893777	0.845718
Difference (%)	1.716	**75.574**
Bi-objective(I point)	0.949116	2.830932
Single-objective($\eta_{ex,r}$)	0.965799	6.061116
Difference (%)	**1.727**	114.103
Term	ΔP (kPa)	Total Cost ($)
Bi-objective (J point)	2.395281	302076
Single-objective (cost)	2.360096	302075
Difference (%)	1.491	**0.003**
Bi-objective (K point)	1.282647	317646.9
Single-objective (ΔP)	0.845718	324896.6
Difference (%)	**51.664**	2.282

Table 9. Comparisons of single-objective results with three-objective optimal design

Term	**$\eta_{ex,r}$**	**ΔP (kPa)**	**Total Cost ($)**
Three -objective(L point)	0.932651	2.60852	302082.8
Single-objective(ΔP)	0.893777	0.845718	324896.6
Difference (%)	4.168	**208.439**	7.552
Three-objective(L point)	0.932651	2.60852	302082.8
Single-objective($\eta_{ex,r}$)	0.965799	6.061116	326967.8
Difference (%)	**3.432**	132.358	8.238
Three-objective(L point)	0.932651	2.60852	302082.8
Single-objective(cost)	0.93249	2.360096	302075
Difference (%)	0.017	10.526	**0.003**

study to obtain a final solution [6]. Accordingly, first, a hypothetical point (ideal point) was defined at which each objective function had the optimum value obtained from the single-objective optimization, as listed in Table 9; as such, these ideal points might not be located on the Pareto-front. Second, all the points on the Pareto-front were normalized as follows [6]:

$$(\Delta P)^* = \frac{\Delta P - (\Delta P)_{min}}{(\Delta P)_{max} - (\Delta P)_{min}} \quad (36)$$

$$(Cost)^* = \frac{Cost - (Cost)_{min}}{(Cost)_{max} - (Cost)_{min}} \quad (37)$$

$$(1/\eta_{ex,r})^* = \frac{1/\eta_{ex,r} - (1/\eta_{ex,r})_{min}}{(1/\eta_{ex,r})_{max} - (1/\eta_{ex,r})_{min}} \quad (38)$$

It should be noted that once finished with the normalization task, the number of ideal points changed to zero. The final optimal solution was defined as the closest design point on the Pareto-front to the ideal point.

Figure 12 shows the normalized Pareto-front obtained in the course of the exergy-economic optimization. As shown in Fig. 12, the design point E is at the shortest distance to the ideal point, thereby representing the final solution for the Pareto-front.

The normalized Pareto-front obtained in the course of exergy-hydraulic optimization is illustrated in Fig. 13. This figure indicates that the design point H is the nearest design point to the ideal point, thereby representing the final solution for this Pareto-front.

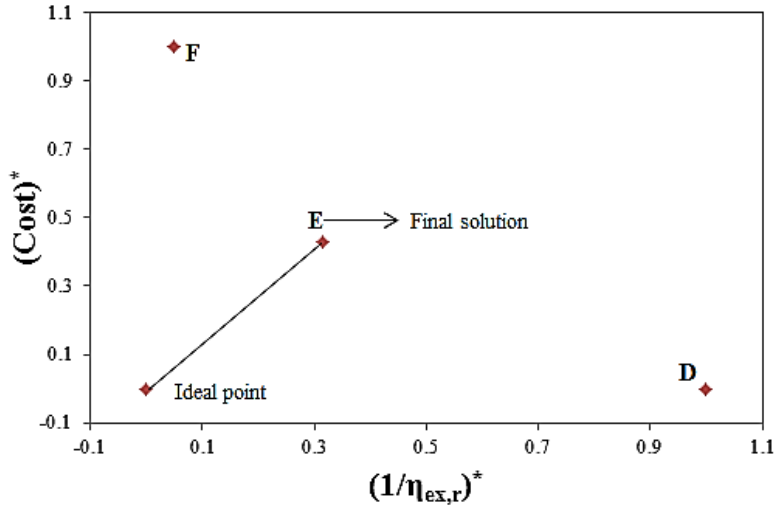

Fig. 12. Normalized Pareto-optimal front for exergy-economic optimization

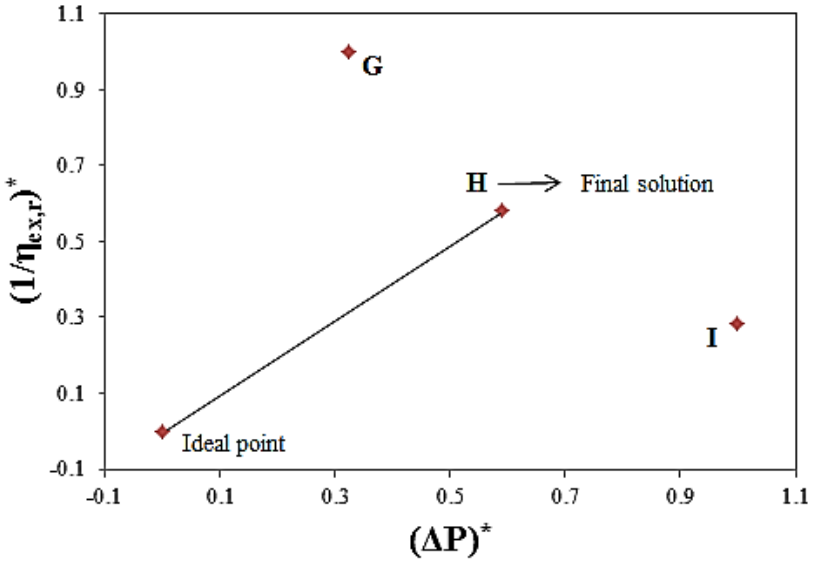

Fig. 13. Normalized Pareto-optimal front for exergy-hydraulic optimization

The normalized Pareto-front obtained in the course of the economic-hydraulic optimization is shown in Fig. 14. The figure illustrates that the design point J, rather than the design point K, is at a shorter distance to the ideal point; therefore, it is considered the final solution for this Pareto-front.

6.Conclusion

In this research, a thermo-hydraulic analysis based on $\varepsilon - NTU$ model was performed for a plate-fin recuperator applied in a 200 kW microturbine with offset strip fin and counter-flow arrangement. The recuperator exergy efficiency, the pressure drop, and the total cost were the important parameters to be optimized using GA and NSGA-II. Six decision variables were considered for the optimizations, and they were fin pitch, fin height, fin offset length, recuperator flow length, recuperator width, and recuperator height. The feasible ranges of pressure drop, Reynolds number and energy efficiency were considered the optimizations' constraints added to the objective functions as a penalty function. The following are the major conclusions drawn:

1. The objective functions were subjected to single-objective optimization via GA; the optimum values of exergy efficiency, pressure drop and total cost were found to be 0.966, 0.846 kPa and 302,075$ respectively.
2. The Pareto-optimal-fronts of bi-objective optimizations (i.e. exergy efficiency-total cost, exergy efficiency-pressure drop, and total cost - pressure drop) were obtained with the design points at which the constraints were determined as being satisfied. On the other hand, the Pareto-fronts obtained clearly showed the contrast between the two objectives for each optimization case.
3. A 3-D Pareto-optimal front was presented for the three-objective optimization with the aforesaid objectives. The only acceptable design point (in terms of the constraints) was specified.
4. The single-objective results were compared to the multi-objective optimum designs. According to the comparisons, exergy efficiency, total cost and pressure drop exhibited maximum differences of 3.432%, 0.001% and 208.439% respectively, between the two optimization approaches. The large difference observed in the case of pressure drop was due to the corresponding constraint.
5. A normalization decision-making approach was followed to achieve the final optimal solution. For exergy efficiency-total cost optimization, the final optimal design resulted in an exergy efficiency of 0.955 and a total cost of 311,510.8$. The optimum exergy efficiency and the pressure drop were found to be 0.932 and 2.013 kPa respectively under the exergy efficiency-pressure drop optimization-oriented decision-making. The total cost-pressure drop optimization resulted in a total cost of 302,076$ and a pressure drop of 2.395281 kPa, as its final optimal solution.

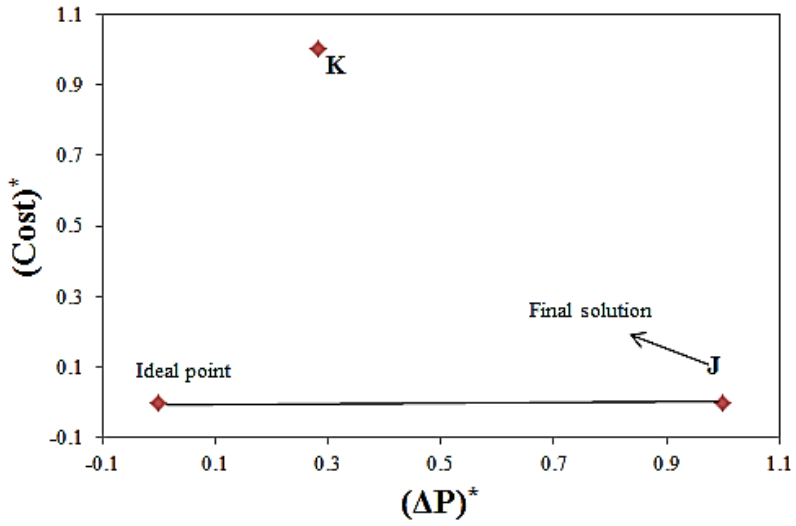

Fig. 14. Normalized Pareto-optimal front for hydraulic-economic optimization

References

[1] Omatete O. O., Maziasz P. J., Pint B. A., Stinton D. P., Assessment of Recuperator Materials for Microturbines, ORNL/TM-2000/304 (2000).

[2] Shah R. K., Compact Heat Exchangers for Microturbines, in The Fifth Conference on Enhanced, Compact and Ultra-Compact Heat Exchangers: Science, Engineering and Technology, Rochester Institute of Technology, Rochester, New York, USA(2005).

[3] Qiuwang W., Hongxia L., Gongnan X., Min Z., Laiqin L., ZhengPing F., Genetic Algorithm Optimization for Primary Surfaces Recuperator of Microturbine, Journal of Engineering for Gas Turbines and Power (2006) 129 (2): 436-442.

[4] Traverso A., Massardo A. F., Optimal Design of Compact Recuperators for Microturbine Application, Applied Thermal Engineering (2005) 25 (14): 2054-2071.

[5] Xie G. N., Sunden B., Wang Q. W., Optimization of Compact Heat Exchangers by a Genetic Algorithm, Applied Thermal Engineering (2008) 28 (8): 895-906.

[6] Wang Z., Li Y., Irreversibility Analysis for Optimization Design of Plate Fin Heat Exchangers Using a Multi-Objective Cuckoo Search Algorithm, Energy Conversion and Management (2015) 101:126-135.

[7] Kays W. M., London A. L., Compact Heat Exchangers, McGraw-Hill, New York, USA (1984).

[8] Utriainen E., Investigation of Some Heat Transfer Surfaces for Gas Turbine Recuperators, Ph.D. Thesis, Division of Heat Transfer, Department of Heat and Power Engineering, Lund Institute of Technology, Lund, Sweden (2001).

[9] Manglik R. M., Bergles A. E., Heat Transfer and Pressure Drop Correlations for the Rectangular Offset Strip Fin Compact Heat Exchanger, Experimental Thermal and Fluid Science (1995) 10 (2): 171-180.

[10] Zhenyu L., Huier C., Multi-Objective Optimization Design Analysis of Primary Surface Recuperator for Microturbine, Applied Thermal Engineering (2008) 28 (5): 601-610.

[11] Peng H., Ling X., Optimal Design Approach for the Plate-Fin Heat Exchangers Using Neural Networks Cooperated with Genetic Algorithms, Applied Thermal Engineering (2008) 28 (5): 642-650.

[12] Sanaye S., Hajabdollahi H., Thermal-Economic Multi-Objective Optimization of Plate Fin Heat Exchanger Using Genetic Algorithm, Applied Energy (2010) 87 (6): 1893-1902.

[13] Ahmadi P., Hajabdollahi H., Dincer I., Cost and Entropy Generation Minimization of a Cross-Flow Plate Fin Heat Exchanger Using Multi-Objective Genetic Algorithm, Journal of Heat Transfer (2011) 133 (2): 021801.

[14] Najafi H., Najafi B., Hoseinpoori P., Energy and Cost Optimization of a Plate and Fin Heat Exchanger Using Genetic Algorithm, Applied Thermal Engineering (2011) 31 (10): 1839-1847.

[15] Shah R. K., Sekulic D. P., Fundamentals of Heat Exchanger Design, John Wiley & Sons, Hoboken, New Jersey, USA (2003).

[16] Rostami A. A., Design of Heat Exchangers, Jahad Daneshgahi of Isfahan University of Technology (1994).

[17] Kaviri A. G., Jaafar M. N. M., Lazim T. M., Modeling and Multi-Objective Exergy Based Optimization of a Combined Cycle Power Plant Using a Genetic Algorithm, Energy Conversion and Management (2012) 58: 94-103.

[18] Energy Efficiency Best Practice Programme, Compact Heat Exchangers, A Training Package for Engineers, UK, ESTU, WS Atkins Consultants Ltd (2000).

[19] Bejan A., Tsatsaronis G., Moran M. J., Thermal Design and Optimization, John Wiley & Sons, Hoboken, New Jersey, USA (1996).

[20] Oskonejad M. M., Engineering Economy, Amirkabir University of Thechnology, Tehran, Iran (1998).

[21] Sadeghi S., Saffari H., Bahadormanesh N., Optimization of a Modified Double-Turbine Kalina Cycle by Using Artificial Bee Colony algorithm, Applied Thermal Engineering (2015) 91: 19-32.

[22] Feng Y., Zhang Y., Li B., Yang J., Shi Y., Comparison Between Regenerative Organic Rankine Cycle (RORC) and Basic Organic Rankine Cycle (BORC) Based on Thermoeconomic Multi-Objective Optimization Considering Exergy Efficiency and Levelized Energy Cost (LEC), Energy Conversion and Management (2015)96: 58-71.

[23] Sadeghzadeh H., Ehyaei M. A., Rosen

M. A., Techno-Economic Optimization of a shell and tube heat exchanger by genetic and particle swarm algorithms, Energy Conversion and Management (2015)93: 84-91.

[24] Golberg D. E., Genetic Algorithms in Search, Optimization, and Machine Learning, Addion Wesley (1989).

[25] Ahmadi M. H., Mohammadi A. H., Feidt M., Pourkiaei S. M., Multi-Objective Optimization of an Irreversible Stirling Cryogenic Refrigerator Cycle, Energy Conversion and Management (2014)82: 351-360.

[26] Schaffer J. D., Multiple Objective Optimization with Vector Evaluated Genetic Algorithms, in Proceedings of the 1st International Conference on Genetic Algorithms, Pittsburgh, USA (1985) 93-100.

[27] Srinivas N., Deb K., Muiltiobjective Optimization Using Nondominated Sorting in Genetic Algorithms, Evolutionary Computation (1994) 2 (3): 221-248.

[28] Deb K., Pratap A., Agarwal S., Meyarivan T., A Fast and Elitist Multiobjective Genetic Algorithm, NSGA-II, Evolutionary Computation (2002) 6 (2): 182-197.

[29] Deb K., Goel T., Controlled Elitist Non-Dominated Sorting Genetic Algorithms for Better Convergence, Evolutionary Multi-Criterion Optimization 1993 (2001) 67-81.